DYNAMICAL CHAOS AND NONEQUILIBRIUM STATISTICAL MECHANICS

PIERRE GASPARD
Université Libre de Bruxelles,
Center for Nonlinear Phenomena and Complex Systems,
Campus Plaine, Code Postal 231,
B-1050 Brussels, Belgium
E-mail: gaspard@ulb.ac.be

Chaos in the motion of atoms and molecules composing fluids is a new topic in nonequilibrium physics. Relationships have been established between the characteristic quantities of chaos and the transport coefficients thanks to the concept of fractal repeller and the escape-rate formalism. Moreover, the hydrodynamic modes of relaxation to the thermodynamic equilibrium as well as the nonequilibrium stationary states have turned out to be described by fractal-like singular distributions. This singular character explains the second law of thermodynamics as an emergent property of large chaotic systems. These and other results show the growing importance of ephemeral phenomena in modern physics.

1 Introduction

The vast majority of natural phenomena are transient processes we could call *ephemeral phenomena*. Examples of such phenomena are the unimolecular reactions and the decays of radioactive nuclei or unstable particles. At the macroscopic level, the irreversible processes of relaxation toward the thermodynamic equilibrium also provide examples of ephemeral phenomena. These transient processes are characterized by a lifetime or a relaxation time associated with an exponential decay. Such exponential decays seem *a priori* incompatible with a microscopic time evolution which is time-reversal symmetric as it is the case for almost all known forces of nature. But theoretical advances have shown that these exponential decays are the natural feature of time-reversible quantum or classical dynamical systems.

In quantum mechanics, scattering theory[1] has already shown that exponential decays of the wavefunction can be understood in terms of poles of the scattering matrix at complex energies $E_r = \varepsilon_r - i\Gamma_r/2$.[2] These poles are associated with quantum resonances appearing in the scattering cross-sections or in other signals measured in a scattering experiment. The lifetime of these quantum resonances is given in terms of the imaginary part of the energy according to $\tau_r = \hbar/\Gamma_r$. These quantum resonances provide a fundamental interpretation for the one-particle decay processes in nuclear, atomic and

molecular reactions.

Less known is the possibility of very similar considerations in classical mechanics, where exponential decays also exist.[3] Examples are here the classical motion of a particle in a potential with a maximum point such as in the inverted harmonic potential. The motion near a typical maximum point is dynamically unstable, leading to an exponential decay of statistical ensembles of trajectories, as shown below. The dynamical instability or sensitivity to the initial conditions is characterized by the rate of exponential separation between initially close trajectories. This rate is called a *Lyapunov exponent*,[4] which turns out to be equal to the rate of exponential decay in the given example. In more complicated potentials, the dynamical instability also generates a dynamical randomness which is called *chaos*. Recent work has revealed that such results are of great importance to understand relaxation processes in statistical mechanics.

On the one hand, many studies have shown that typical systems of statistical mechanics are dynamically unstable with a full spectrum of positive Lyapunov exponents, one for each unstable perturbation on the trajectories of these many-body systems.[5,6,7,8,9,10,11,12,13,14] This microscopic chaos occurs on a time scale corresponding to the intercollisional time between the particles composing the fluid, which is of the order of 10^{-10} sec in a gas at room temperature and pressure. In this regard, we should distinguish the microscopic chaos from the macroscopic one. This latter evolves on the much longer time scale of the hydrodynamic collective motions of the fluid,[4,15] although the microscopic chaos drives the thermal fluctuations and the other stochastic processes such as Brownian motion (see below).[3]

On the other hand, quantitative relationships have been discovered between the characteristic quantities of the microscopic chaos and the transport coefficients.[16,17,18,19,20] The basis of such relationships is the existence of exponentially decaying nonequilibrium states which have fractal properties generated by the microscopic chaos. These nonequilibrium fractal structures have been discovered in different approaches[18,19] and, in particular, in the escape-rate formalism[17,21,22,23] and in the related Liouville-equation approach.[3,24,25]

The escape-rate formalism is a scattering theory of transport in which a nonequilibrium state is defined by the set of unstable trajectories forever trapped in a finite domain of the space of the positions and velocities of all the particles (the so-called *phase space*). These trapped trajectories form a *fractal repeller*.[3] Since most trajectories do not remain trapped the fractal repeller is characterized by a rate of exponential decay called the *escape rate*. This rate is related, on the one hand, to the transport coefficients and, on the other hand, to the characteristic quantities of chaos, hence the relationships

between these quantities.[17,21,22,23]

The Liouville-equation approach considers the exponential relaxation toward equilibrium in a closed system without escape. This relaxation is described by the so-called *hydrodynamic modes*, of which several approximations are known.[26,27,28] The crudest approximation is the one given at the hydrodynamic level of description by the linearized Navier-Stokes equations. For dilute fluids, more detailed approximations are given at the kinetic level of description by the solutions of the linearized Boltzmann equation. However, until recently, no exact solution has been known for the hydrodynamic modes. The study of simple models of diffusion such as the multibaker map and the Lorentz gases has shown that the hydrodynamic modes are not defined by regular distributions with a density function, but by singular distributions without density function.[3,24,25] Moreover, these singular distributions have fractal properties originating from the microscopic chaos. As a corollary of their singular character, these distributions have the remarkable property to relax exponentially under the deterministic microscopic dynamics (see below).

A most remarkable result is that the fractal-like singular character of the hydrodynamic modes provides an explanation for the second law of thermodynamics. Indeed, it has been possible to show explicitly on simple models of diffusion that the entropy production is positive and has the value expected from nonequilibrium thermodynamics because of the fractal-like singular character of the hydrodynamic modes.[29,30]

The purpose of the present paper is to review these new results of nonequilibrium statistical mechanics and to place them in a broader perspective.

This review is organized as follows. The basic properties of microscopic chaos are described in Sec. 2. The methods of statistical mechanics which allow the determination of the classical resonances of the Liouville equation are presented in Sec. 3. Section 4 gives a summary of the scattering theory of transport which is the escape-rate formalism. The recent results on the hydrodynamic modes and the nonequilibrium steady states are summarized in Secs. 5 and 6, respectively. The consequences of these results to the problem of the second law of thermodynamics are discussed in Sec. 7. Conclusions and perspectives are drawn in Sec. 8.

2 Microscopic chaos

Since Newton, the time evolution of systems of interacting particles is described by differential equations. For fluids or solids at room temperature and pressure, classical mechanics constitutes an excellent approximation for the motion of atoms and molecules. If the system is composed of N particles

at positions $\mathbf{r}_i$ and momenta $\mathbf{p}_i$, moving in a d-dimensional physical space, the state of the system follows a trajectory in the $2dN$-dimensional phase space of coordinates $\mathbf{X} = (\mathbf{r}_1, \mathbf{p}_1, \mathbf{r}_2, \mathbf{p}_2, ..., \mathbf{r}_N, \mathbf{p}_N)$. According to classical mechanics, the motion of the particles is determined by Hamilton's equations

$$\begin{cases} \dfrac{d\mathbf{r}_i}{dt} = +\dfrac{\partial H}{\partial \mathbf{p}_i} \ , \\ \dfrac{d\mathbf{p}_i}{dt} = -\dfrac{\partial H}{\partial \mathbf{r}_i} \ , \end{cases} \tag{1}$$

in terms of the so-called *Hamiltonian function* $H(\mathbf{X})$.

2.1 Dynamical instability

The trajectory of the system is uniquely determined by the knowledge of the initial conditions, but the predictability of the Newtonian scheme is affected by the possible instability of the trajectories. Indeed, the initial conditions are always known with some error bar which may amplify during the time evolution if the trajectory is unstable. This possible dynamical instability is studied by linearizing Hamilton's equations (1). If $\mathbf{F}(\mathbf{X})$ denotes the Hamiltonian vector field in the right-hand side of Eqs. (1), the trajectory $\mathbf{X}_t$ and its infinitesimal perturbation $\delta\mathbf{X}_t$ evolve according to

$$\begin{cases} \dfrac{d\mathbf{X}_t}{dt} = \mathbf{F}(\mathbf{X}_t) \ , \\ \dfrac{d}{dt}\delta\mathbf{X}_t = \dfrac{\partial \mathbf{F}}{\partial \mathbf{X}}(\mathbf{X}_t) \cdot \delta\mathbf{X}_t \ . \end{cases} \tag{2}$$

The trajectory is unstable if the infinitesimal perturbation grows exponentially in time and, therefore, if the so-called *Lyapunov exponent*:

$$\lambda = \lim_{t\to\infty} \frac{1}{t} \ln \frac{\|\delta\mathbf{X}_t\|}{\|\delta\mathbf{X}_0\|} \ , \tag{3}$$

is positive. There exist as many Lyapunov exponents as there are linearly independent initial perturbations $\delta\mathbf{X}_0$. Since the dimension of the space of the perturbations $\delta\mathbf{X}$ is equal to the dimension of the phase space, there are $2dN$ Lyapunov exponents which form the so-called *Lyapunov spectrum*:[4]

$$\lambda_{\max} = \lambda_1 \geq \lambda_2 \geq \cdots \geq 0 \geq \cdots \geq \lambda_{\min} \ . \tag{4}$$

In Hamiltonian systems, the symplectic character of the vector field $\mathbf{F}(\mathbf{X})$ implies that the Lyapunov exponents appear in pairs $\{+\lambda_i, -\lambda_i\}$, which is

known as the Hamiltonian *pairing rule*.[3] As a consequence, the sum of all the Lyapunov exponents vanishes $\sum_i \lambda_i = 0$ in accordance with Liouville's theorem which guarantees the preservation of phase-space volumes under a Hamiltonian time evolution.

Numerical methods have been developed to compute the Lyapunov exponents and the Lyapunov spectrum of many-particle systems has been obtained for fluids, solids, or plasmas.[8,9,10]

Fig. 1 depicts the spectrum of the non-negative Lyapunov exponents for a hard-disk model of Brownian motion.[31] In this two-dimensional model, the system is composed of a large disk surrounded by many small disks. The large disk represents a heavy colloidal particle in a fluid. The total number of disks is here equal to $N = 64$ so that the phase-space dimension is $4N = 256$. As a consequence of the conservation of total momenta and energy, 6 Lyapunov exponents are zero. Fig. 1 shows that $2N - 3 = 125$ Lyapunov exponents are positive which is a typical situation as observed in many studies.[8,9,10] In Fig. 1, we furthermore observe that the Lyapunov exponents increase with the diameter of the Brownian particle.

In a dilute gas, the typical value of a Lyapunov exponent can be estimated as shown in Fig. 2. If the particles have the diameter d, the mean velocity v, and the mean free path ℓ, a perturbation by an angle $\delta\theta$ on the velocity of a particle just after a collision is amplified at the next collision according to

$$\delta\theta' \ \sim \ \delta\theta \ \frac{\ell}{d} \ . \tag{5}$$

During a time t, the particle undergoes about vt/ℓ collisions so that the perturbation is amplified by a factor which grows exponentially with time as

$$\delta\theta_t \ \sim \ \delta\theta_0 \left(\frac{\ell}{d}\right)^{vt/\ell} \ \sim \ \exp(\lambda t) \ . \tag{6}$$

Accordingly, a typical Lyapunov exponent is given by Krylov's formula[5,7]

$$\lambda \ \sim \ \frac{v}{\ell} \ln \frac{\ell}{d} \ \sim \ 10^{10} \text{ digits/sec} \ , \tag{7}$$

as recently confirmed by kinetic theory.[11,14]

This dynamical instability may generate the escape of trajectories out of an open system, as well as a dynamical randomness of deterministic origin.

2.2 Dynamical randomness

The dynamical randomness is the disorder that the trajectory of the system presents as a function of time. This time disorder is characterized by an

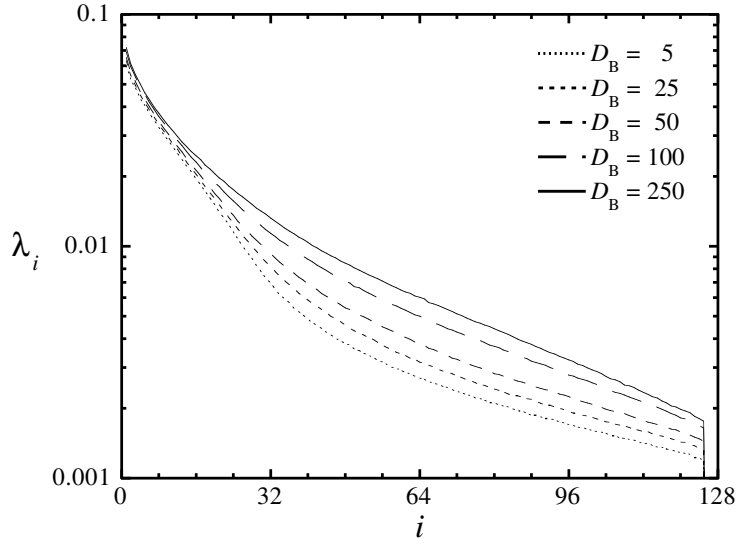

Figure 1. Spectrum of positive Lyapunov exponents for a system of one hard disk of diameter $D_{\rm B}$ and of 63 hard disks of unit diameter. The density of the surrounding fluid is here $n = 10^{-3}$. The Lyapunov exponents increase with the diameter $D_{\rm B}$ of the Brownian particle.

entropy per unit time introduced by Kolmogorov and Sinai[4,32,33] who were inspired by Shannon's work on information theory.[34] The entropy per unit time is the rate of production of information during the coarse-grained stroboscopic observation of a system. This observation is performed by a measuring device which records the instantaneous state of the system by an integer number ω with a sampling time Δt. To each integer ω corresponds a cell C_ω in the phase space of the system. That the measuring device records the number ω_n at time $t_n = n\Delta t$ means that the trajectory visits the corresponding cell at that time: $\mathbf{X}_{t_n} \in C_{\omega_n}$. If the cells are disjoint (i.e., $C_\omega \cap C_{\omega'} = \emptyset$ if $\omega \neq \omega'$) they form a so-called *partition* $\mathcal{P}$ of the phase space. This partition characterizes the measuring device used to observe the system. The stroboscopic observation records the classical history of the system by the sequence of cells visited $\omega_0\omega_1\omega_2\cdots\omega_n\cdots$. The rate $h_{\mathcal{P}}$ of production of information is given by the decay rate of the multiple-time probability[3]

$$\mathrm{Prob}\{\omega_0\omega_1\omega_2\omega_3\cdots\omega_{n-1}\} \sim \exp(-n\ \Delta t\ h_{\mathcal{P}})\ , \tag{8}$$

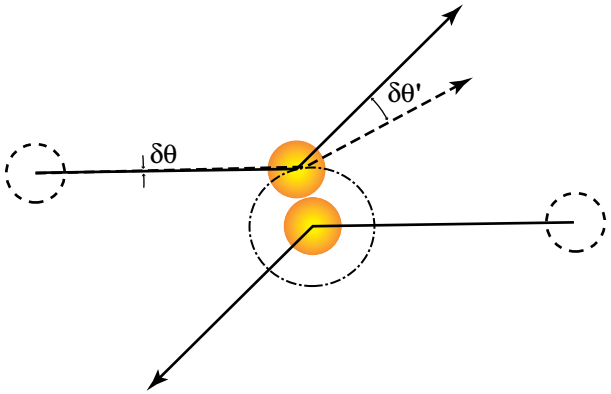

Figure 2. Geometry of a collision between two particles and growth of a perturbation on the velocity of a particle: $\delta\theta \to \delta\theta'$.

as the number n of times increases, $n \to \infty$.

In order to characterize intrinsically the dynamics of the system independently of the measuring device, Kolmogorov and Sinai have considered the supremum of all the rates $h_{\mathcal{P}}$ over all the possible measuring devices, i.e., over all the possible coarse-graining $\mathcal{P}$ of the phase space and they defined the so-called *Kolmogorov-Sinai (KS) entropy per unit time*:[32,33]

$$h_{\rm KS} = {\rm Sup}_{\mathcal{P}}\ h_{\mathcal{P}}\ , \tag{9}$$

Later, the connection between the dynamical instability and randomness was established with the formula [4,35,36]

$$h_{\rm KS} = \sum_{\lambda_i > 0} \lambda_i - \gamma\ , \tag{10}$$

where γ is the so-called *escape rate* of trajectories out of an open system, as considered in the processes of chaotic scattering.[3] When the system is closed, the escape rate vanishes, $\gamma = 0$, and Eq. (10) reduces to Pesin's formula.[37] Therefore, the formula (10) shows that the dynamical instability may generate dynamical randomness and escape:

$$\begin{array}{ccc} & \text{dynamical instability} & \\ & \swarrow \qquad \searrow & \\ \text{dynamical randomness} & & \text{escape} \end{array}$$

For a mole of dilute gas in a closed container, the escape rate vanishes and the KS entropy per unit time can be estimated by multiplying the typical

Lyapunov exponent (7) by the expected total number of positive Lyapunov exponents, which is of the order of three times the Avogadro number so that

$$h_{\rm KS} \ \sim \ 3\, N_{\rm Avogadro}\, \lambda \ \sim \ 10^{34} \ \text{digits/sec mole} \ , \tag{11}$$

for a gas at room temperature and pressure.[7] This estimation has recently been confirmed by kinetic theory.[12] Accordingly, the dynamical randomness is huge for the microscopic motion of the particles in a fluid at room temperature. This KS entropy is the rate of production of information that would be required if we wished to trace all the particles in the fluid. In this sense, it characterizes the microscopic chaos.

In the example of Brownian motion,[31] the KS entropy is given by the area below the curve of the Lyapunov spectrum in Fig. 1 and, as a consequence, the KS entropy increases with the diameter of the Brownian particle. The huge dynamical randomness due to the many positive Lyapunov exponents is at the origin of the erratic character of the Brownian motion itself. Indeed, the Brownian motion is characterized by an entropy per unit time associated with the sole observation of the Brownian particle with a spatial resolution ε.[38] This ε-entropy per unit time $h_{\mathcal{P}_\varepsilon}$ has been measured in a recent experiment,[39] which showed that this entropy is positive and scales like $\mathcal{D}/\varepsilon^2$ where $\mathcal{D}$ is the diffusion coefficient of the Brownian particle. According to the definition (9), this ε-entropy is a small fraction of the KS entropy $h_{\rm KS} = \sum_{\lambda_i > 0} \lambda_i$ and, thus, a small fraction of the area below the Lyapunov spectrum shown in Fig. 1. For such a model of Brownian motion, the ε-entropy is thus some fraction of the sum of positive Lyapunov exponents generated by the internal microscopic dynamics. The same result holds for the model of a Rayleigh flight in a finite box, which is obtained in the limit where the small disks reduce to point particles only interacting with the large disk.

We remark that, in systems without Lyapunov exponents, the KS entropy or its quantum generalizations[40,41] can alone be used to define chaos instead of positive Lyapunov exponent, as discussed elsewhere for lattice gas automata[23] and quantum systems.[42] In support of this proposition, we notice that there exist open non-chaotic systems with a positive Lyapunov exponent but a zero KS entropy and for which the escape rate is given by $\gamma = \lambda$ (see below). A classification of the processes of statistical mechanics in terms of their entropy per unit time has been carried out elsewhere.[3,38]

3 Statistical mechanics and exponential decay

3.1 Statistical ensembles

We could compare statistical mechanics to a computer. A computer has a hardware which cannot be changed. On this hardware, different softwares can run. Each software must be compatible with the hardware but there is no limit to the variety of different softwares beside this constraint of compatibility. Statistical mechanics is similar as it is built on the basis of a given mechanics of particles which cannot be changed.

One of the extra-mechanical assumptions introduced by statistical mechanics is the concept of statistical ensemble of trajectories which can be motivated by different reasons. One reason is that the initial conditions of an experiment are in general not fully reproducible so that slight differences may appear from one experiment to the next. These differences may be due to the preparation of the initial conditions, which depends in general on other systems surrounding the system under study. The uncertainties on the initial conditions acquire a great importance if the system is chaotic because of the high sensitivity of its trajectories to the initial conditions.[15] The purpose of statistical mechanics is to study the statistical properties which emerge – such as the probability law of large numbers – after repeating many times the same experiment. In nonequilibrium statistical mechanics, the statistical properties of interest are dynamical so that a typical experiment consists in observing the time evolution of the system between an initial time $t = 0$ and a final time t.

This time evolution is known in principle as soon as we know the trajectories $\mathbf{X}_t = \mathbf{\Phi}^t \mathbf{X}_0$ which are the solutions of the equations of motion (1). If we have a statistical ensemble of such trajectories $\{\mathbf{X}_t^{(m)}\}_{m=1}^{\infty}$, a probability density can be defined by

$$f_t(\mathbf{X}) \;=\; \lim_{M\to\infty} \; \frac{1}{M} \; \sum_{m=1}^{M} \; \delta\left(\mathbf{X} - \mathbf{X}_t^{(m)}\right) \;, \tag{12}$$

which allows us to evaluate the mean values of the observable quantities $A(\mathbf{X})$ as

$$\langle A \rangle_t \;=\; \int \; A(\mathbf{X}) \; f_t(\mathbf{X}) \; d\mathbf{X} \;. \tag{13}$$

3.2 Liouville equation

The time evolution of the probability density (12) is induced by the mechanical law (1) in a similar way as a software is driven by the underlying hardware. Accordingly, the probability density obeys the *Liouville equation*[15,43]

$$\frac{\partial f_t}{\partial t} \;=\; \hat{L}\; f_t \;, \tag{14}$$

where the so-called *Liouvillian operator* takes one of the following forms:

$$\text{general system :} \qquad \hat{L}f = -\mathrm{div}(\mathbf{F}f) \;, \tag{15}$$

$$\text{Hamiltonian system :} \qquad \hat{L}f = \{H, f\}_{\text{Poisson}} \;, \tag{16}$$

where $\{\cdot,\cdot\}_{\text{Poisson}}$ denotes the Poisson bracket.

The time integral of the Liouville equation gives the probability density at the current time t in terms of the initial density as

$$f_t(\mathbf{X}) \;=\; \exp(\hat{L}t)\; f_0(\mathbf{X}) \;\equiv\; \hat{P}^t f_0(\mathbf{X}) \;, \tag{17}$$

which defines the *Frobenius-Perron operator*. This operator has one of the following forms:

$$\text{general system :} \qquad \hat{P}^t f(\mathbf{X}) = \frac{f(\mathbf{\Phi}^{-t}\mathbf{X})}{\left|\dfrac{\partial \mathbf{\Phi}^t}{\partial \mathbf{X}}\left(\mathbf{\Phi}^{-t}\mathbf{X}\right)\right|} \;, \tag{18}$$

$$\text{Hamiltonian system :} \qquad \hat{P}^t f(\mathbf{X}) = f(\mathbf{\Phi}^{-t}\mathbf{X}) \;. \tag{19}$$

We notice that $\left|\dfrac{\partial \mathbf{\Phi}^t}{\partial \mathbf{X}}\right| = 1$ for Hamiltonian systems because they preserve the phase-space volumes, hence Eq. (19).

We remark that various kinds of boundary conditions can be imposed on the solutions of the Liouville equation whether the system is at the thermodynamic equilibrium or out of equilibrium, in a similar way as boundary conditions are needed to solve the Navier-Stokes and Boltzmann equations.[3,44]

3.3 Time asymptotics

The relaxation toward an equilibrium or nonequilibrium thermodynamic state is a phenomenon occurring in the limit of long times, $t \to \infty$. Methods have been developed in order to expand the mean values (13) asymptotically in time. These asymptotic expansions are controlled by the so-called Pollicott-Ruelle resonances[45,46,47,48,49,50] and the other singularities of the Liouvillian resolvent at complex frequencies.

An example of such asymptotic expansion is given by

$$\langle A\rangle_t = \langle A|\hat{P}^t|f_0\rangle \simeq_{t\to+\infty} \langle A|\Psi_{\rm st}\rangle\langle\tilde{\Psi}_{\rm st}|f_0\rangle + \sum_i \exp(-\gamma_i t)\langle A|\Psi_i\rangle\langle\tilde{\Psi}_i|f_0\rangle + \cdots \ , \tag{20}$$

with possible contributions from branch cuts or other complex singularities as well as Jordan-block structures[3] since the Frobenius-Perron operator is not unitary. In dynamically unstable systems, the Pollicott-Ruelle resonances $\{\gamma_i\}$ can be obtained as the zeros of the Selberg-Smale zeta function, as shown by periodic-orbit theory.[51,52,53,54] Pollicott-Ruelle resonances have also been experimentally observed in hard-disk scatterers.[55]

The states appearing in the expansion (20) are the right- and left-eigenstates of the Frobenius-Perron operator:

$$\hat{P}^t\Psi_i \ = \ \exp(-\gamma_i t)\ \Psi_i \ , \tag{21}$$

$$\hat{P}^{t\dagger}\tilde{\Psi}_i \ = \ \exp(-\gamma_i^* t)\ \tilde{\Psi}_i \ , \tag{22}$$

which differ in general because the Frobenius-Perron operator is non-unitary. The first term in Eq. (20) contains the stationary state. If this stationary state is unique the system is ergodic. If moreover Re $\gamma_i > 0$ for all the resonances and other singularities, the system is mixing. In general, the eigenstates are not given by functions but by Gel'fand-Schwartz distributions,[56,57] as shown by the following example.

3.4 Particle moving on a hill

As a simple example of time asymptotics,[3] let us consider a particle moving in a one-dimensional potential under the Hamiltonian

$$H = \frac{p^2}{2m} + V(r) \ . \tag{23}$$

The potential $V(r)$ is supposed to have a maximum at $r = 0$ and to become constant at large distances $r \to \pm\infty$ (see Fig. 3a).

This system presents a dynamical instability without chaos. Indeed, the particle remains at the top of the hill if it has no momentum, so that $r = p = 0$ is a stationary solution. However, this trajectory is unstable with a positive Lyapunov exponent given by $\lambda = \sqrt{-\frac{1}{m}\frac{\partial^2 V}{\partial r^2}(0)}$. Fig. 3b depicts different trajectories issued from N_0 initial conditions which are very close to the point $r = p = 0$. Fig. 3c represents the fraction N_t/N_0 of trajectories which are still in the interval $-a \le r \le +a$ at the current time t. We observe that this fraction decays exponentially at long times. The rate of decay defines the escape rate γ of the hill. Since the trajectories which escape at very long

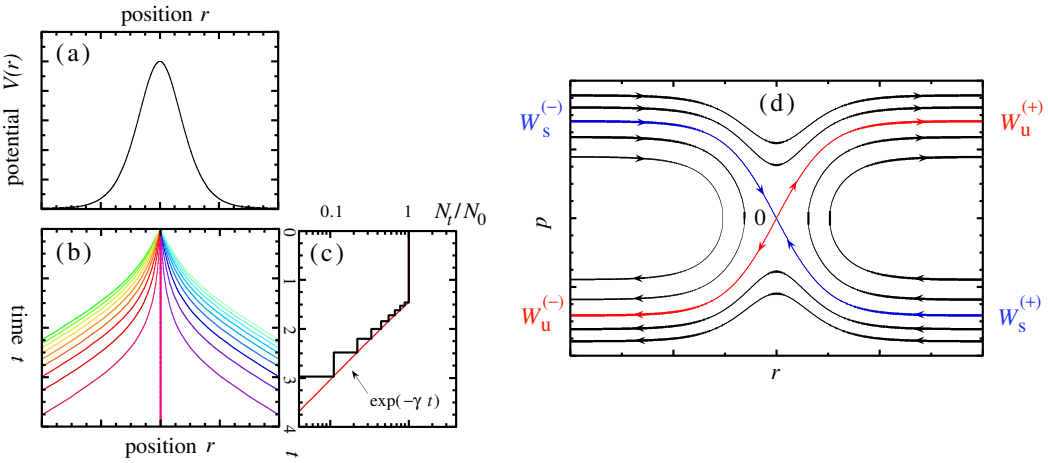

Figure 3. Particle moving down a hill: (a) The potential. (b) Trajectories issued from initial conditions nearby the top $r = 0$. (c) The number N_t of trajectories still on the hill by the time t divided by the initial number of trajectories N_0. The red curve is the curve in the limit $N_0 \to \infty$. (d) Phase portrait of the trajectories in the position-momentum space. $W_{\rm s}^{(\pm)}$ and $W_{\rm u}^{(\pm)}$ denote respectively the stable and unstable manifolds of the point $r = p = 0$.

times are issued from very near the point $r = p = 0$, we can understand that the long-time decay is controlled by the dynamical instability near $r = p = 0$ and, thus, that the escape rate is equal to the Lyapunov exponent: $\gamma = \lambda$. In Fig. 3d, the portrait is drawn of several trajectories of the system in the phase space $\mathbf{X} = (r, p)$. Special trajectories $\mathbf{X}_{\rm s,u}^{(\pm)}(\tau)$ known as the *stable and unstable manifolds* are connected to the stationary solution at $\mathbf{X} = 0$. The signs denote both branches of these manifolds.

For $t \to +\infty$, the probability density tends to concentrate along the unstable manifold. We can check that the distribution

$$\Psi(\mathbf{X}) \;=\; \sum_{\epsilon=\pm} \int_{-\infty}^{+\infty} \exp(\gamma\tau)\; \delta\left[\mathbf{X} - \mathbf{X}_{\rm u}^{(\epsilon)}(\tau)\right]\; d\tau \;, \tag{24}$$

is an exact eigenstate of the Frobenius-Perron operator

$$\hat{P}^t \Psi(\mathbf{X}) \;=\; \Psi(\mathbf{\Phi}^{-t}\mathbf{X}) \;=\; \exp(-\gamma t)\; \Psi(\mathbf{X}) \;, \tag{25}$$

because $\mathbf{\Phi}^t \mathbf{X}_{\rm u}^{(\epsilon)}(\tau) = \mathbf{X}_{\rm u}^{(\epsilon)}(\tau + t)$ and because the flow is area-preserving in the plane of the variables $\mathbf{X} = (r, p)$. The eigenstate (24) is associated with the escape rate $\gamma = \lambda$, which is a generalized eigenvalue of the corresponding Liouvillian operator (16).

This simple example shows that an exponential decay may be considered as an exact property of a classical system if the decaying state is supposed to be a Gel'fand-Schwartz distribution instead of a function. A full asymptotic expansion can be obtained for $t \to \pm\infty$. For $t \to -\infty$, the eigenstates are concentrated on the stable manifold instead of the unstable one. Accordingly, a spontaneous breaking of the time-reversal symmetry appears between both asymptotic expansions, defining two semigroups with distinct domains of application: either $t > 0$ or $t < 0$.

4 Scattering theory of transport

The particle moving on a hill is a simple example of scattering systems with a unique trajectory which is forever trapped at finite distance for $t \to \pm\infty$. Most often, the scattering process is chaotic because the trapped trajectories form an uncountable set which is invariant under the dynamics and which is characterized by a positive KS entropy.[3] If all the trapped trajectories are unstable, the invariant set may be a fractal characterized by positive Lyapunov exponents and an escape rate, which are related to the KS entropy according to Eq. (10). For this so-called fractal repeller, partial information dimensions d_i can be associated with each unstable direction,[4] which allows us to decompose the KS entropy on the spectrum of positive Lyapunov exponents according to $h_{\rm KS} = \sum_{\lambda_i > 0} d_i \lambda_i$. Introducing the partial codimensions as $c_i = 1 - d_i$, Eq. (10) shows that the escape rate has a similar decomposition $\gamma = \sum_{\lambda_i > 0} c_i \lambda_i$. In this framework, a scattering theory of transport can be constructed, which extends an early theory by Lax and Phillips.[58]

A connection to the transport coefficients can be established by noticing that each transport property corresponds to the diffusive motion of the center of one of the conserved quantities in a many-particle system. For instance, viscosity is given by the diffusivity of the center of the momenta of the particles, heat conductivity by the diffusivity of the center of the energies of the particles, diffusion itself by the diffusivity of a tracer particle, etc... The centers of the transport properties are called the Helfand moments (see Table 1).[59] The microscopic current associated with a transport property is given as the time derivative of the Helfand moment: $J^{(\alpha)} = dG^{(\alpha)}/dt$. The transport coefficients can equivalently be expressed either in terms of the microscopic current by the Green-Kubo formula, or the Helfand moment by the

Table 1. Helfand's moments.

process	*moment*
self-diffusion	$G^{(\mathrm{D})} = x_i$
shear viscosity	$G^{(\eta)} = \frac{1}{\sqrt{V k_{\mathrm{B}} T}} \sum_{i=1}^{N} x_i \, p_{iy}$
bulk viscosity ($\psi = \zeta + \frac{4}{3}\eta$)	$G^{(\psi)} = \frac{1}{\sqrt{V k_{\mathrm{B}} T}} \sum_{i=1}^{N} x_i \, p_{ix}$
heat conductivity	$G^{(\kappa)} = \frac{1}{\sqrt{V k_{\mathrm{B}} T^2}} \sum_{i=1}^{N} x_i \, (E_i - \langle E_i \rangle)$
charge conductivity	$G^{(\mathrm{e})} = \frac{1}{\sqrt{V k_{\mathrm{B}} T}} \sum_{i=1}^{N} e Z_i \, x_i$

Einstein formula:[59,60,61]

$$\alpha = \int_0^\infty \langle J_0^{(\alpha)} J_t^{(\alpha)} \rangle dt = \lim_{t \to \infty} \frac{1}{2t} \, \langle (G_t^{(\alpha)} - G_0^{(\alpha)})^2 \rangle \; . \tag{26}$$

Accordingly, each Helfand moment $G_t^{(\alpha)}$ performs a random walk so that the probability density that $G_t^{(\alpha)} = g$ obeys a diffusion equation with the transport coefficient α as diffusion coefficient

$$\frac{\partial p}{\partial t} = \alpha \frac{\partial^2 p}{\partial g^2} \; . \tag{27}$$

A fractal repeller will be defined by selecting the trajectories of the many-particle system for which the Helfand moment associated with the transport property of interest performs its random walk between absorbing boundaries

$$-\frac{\chi}{2} \leq G_t^{(\alpha)} \leq +\frac{\chi}{2} \; , \tag{28}$$

separated by distances large enough with respect to the mean free path. Escape occurs when the Helfand moment reaches the absorbing boundaries. The escape rate can be calculated by solving Eq. (27) with the absorbing boundary conditions $p(\pm\chi/2) = 0$, yielding the solution

$$p(g,t) = \sum_{j=1}^{\infty} a_j \; \exp(-\gamma_j t) \; \sin\left(\frac{j\pi g}{\chi} + \frac{j\pi}{2} \right) \; , \tag{29}$$

with

$$\gamma_j = \alpha \left(\frac{j\pi}{\chi} \right)^2 \; , \qquad \text{and} \quad j = 1, 2, 3, ... \tag{30}$$

The slowest decay rate controls the escape over the longest time scale so that the escape rate can be estimated as

$$\gamma \simeq \gamma_1 = \alpha \left(\frac{\pi}{\chi} \right)^2 , \qquad \text{for} \quad \chi \to \infty . \tag{31}$$

Combining with the formula (10), we obtain a relationship between the transport coefficient and the characteristic quantites of chaos evaluated on the fractal repeller defined by the absorbing boundary conditions at $g = \pm\chi/2$:[17,22]

$$\alpha \; = \; \lim_{\chi, V \to \infty} \left(\frac{\chi}{\pi} \right)^2 \left(\sum_{\lambda_i > 0} \lambda_i - h_{\rm KS} \right)_\chi \; = \; \lim_{\chi, V \to \infty} \left(\frac{\chi}{\pi} \right)^2 \left(\sum_{\lambda_i > 0} c_i \; \lambda_i \right)_\chi . \tag{32}$$

The thermodynamic limit $N, V \to \infty$ (with N/V kept constant) may be necessary to perform before the limit $\chi \to \infty$ because the absorbing boundaries must be contained inside the volume V.

An example is diffusion in the periodic Lorentz gas. In this case, the Helfand moment reduces to the position of the point particle undergoing elastic collisions in a periodic array of hard disks fixed in the plane. Imposing absorbing boundaries is essentially equivalent to removing all the disks outside the region delimited by the boundaries. The point particle escapes to infinity in free motion as soon as the boundaries are reached as illustrated in Fig. 4.[21] This open Lorentz gas is an example of chaotic scattering. Fig. 5 depicts the time that the particle takes to escape as a function of the initial velocity angle. This escape-time function has singularities at each initial condition of a trajectory which is attracted toward the repeller, i.e., belonging to the stable manifold of the repeller. The escape-time function has self-similar properties as revealed by successive zooms depicted in Fig. 5, giving numerical evidence that the repeller is fractal. In this open Lorentz gas, the diffusion coefficient $\mathcal{D}$ is given in terms of the positive Lyapunov exponent λ and the partial Hausdorff dimension $0 \le d_{\rm H}(k) \le 1$ of the fractal repeller by[21]

$$\mathcal{D} = \lambda \; \lim_{k \to 0} \frac{1 - d_{\rm H}(k)}{k^2} , \qquad \text{with} \quad k = \frac{2.67495}{L} , \tag{33}$$

for absorbing boundaries on a hexagon with vertices at the distance L from the center.

The escape-rate formalism can also be considered in the presence of external fields to determine the mobility coefficient such as the charge conductivity.[3] Reaction rates can also be related to the characteristic quantities of chaos thanks to the escape-rate formalism.[62]

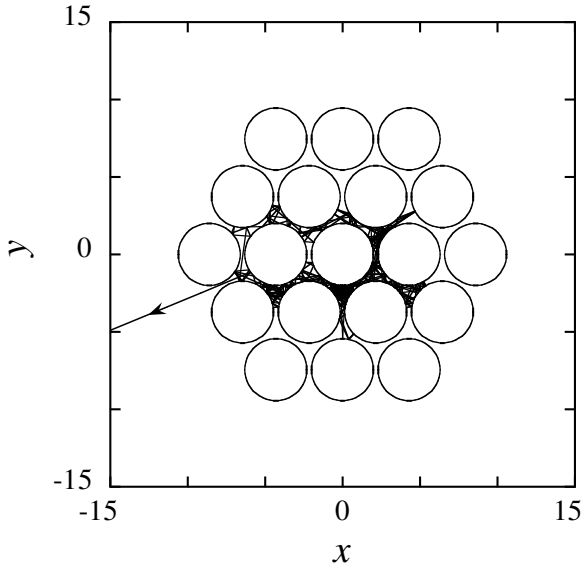

Figure 4. Trajectory of a particle escaping from a hexagonal open Lorentz gas with $L = 2d$ where $d = 2.15a$ is the distance between the centers of the disks and $a = 2$ is their radius. The initial condition is located on the central disk at an angle $\theta = \pi/4$ with respect to the x-axis.

5 Hydrodynamic modes

The hydrodynamic modes are exponentially decaying solutions of Liouville's equation. The remarkable result is that such solutions have been recently constructed in simple chaotic models of diffusion.[3,24,25,63,64,65] These constructions have revealed the singular and fractal character of these hydrodynamic modes, which turn out to be mathematical distributions without a density function, in contrast to what has been commonly assumed in kinetic theory.

The chaotic models which have been considered are the multibaker map[66] and the periodic Lorentz gases with hard-disk scatterers[67,68] or with attractive screened Coulombic scatterers.[69] These systems are periodically extended in space and have a fully chaotic dynamics. The periodic Lorentz gases are

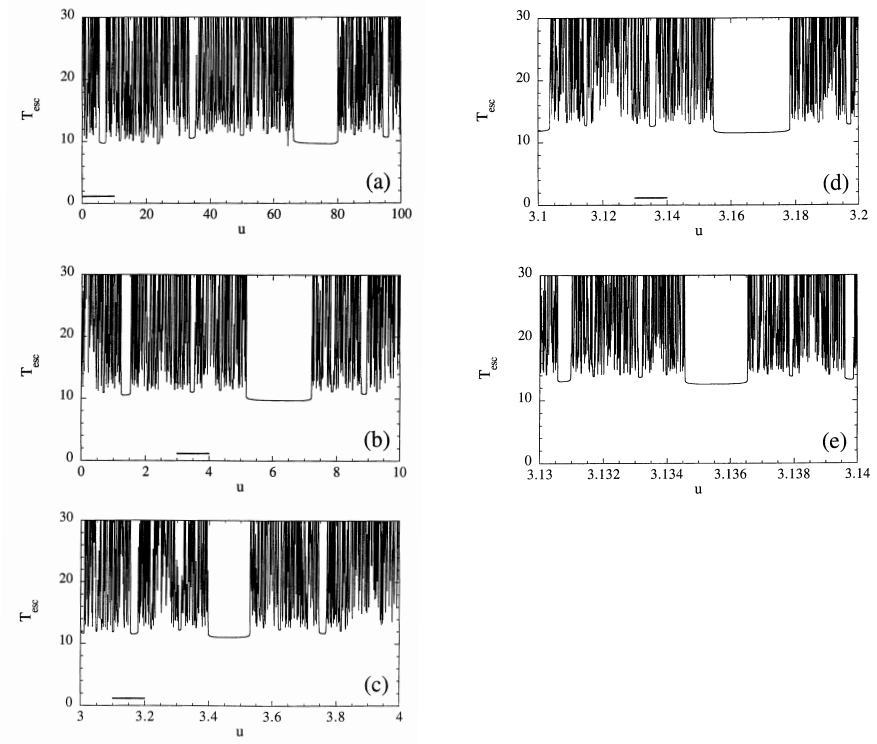

Figure 5. Escape-time function for the open Lorentz gas of Fig. 4. The initial position is always at the angle $\theta = \pi/4$ on the central disk while the initial velocity angle varies according to $\pi u \times 10^{-10}$: (a)-(e) show successive zooms of the function.

described by the Hamiltonian function

$$H = \frac{\mathbf{p}^2}{2m} + \sum_{\mathbf{l}} V(\mathbf{r} - \mathbf{l}) \ , \tag{34}$$

where $\mathbf{l}$ is a vector of the lattice of scatterers and V is a potential which is

$$V = \begin{cases} \infty \ , & r < a \ , \\ 0 \ , & r > a \ , \end{cases} \tag{35}$$

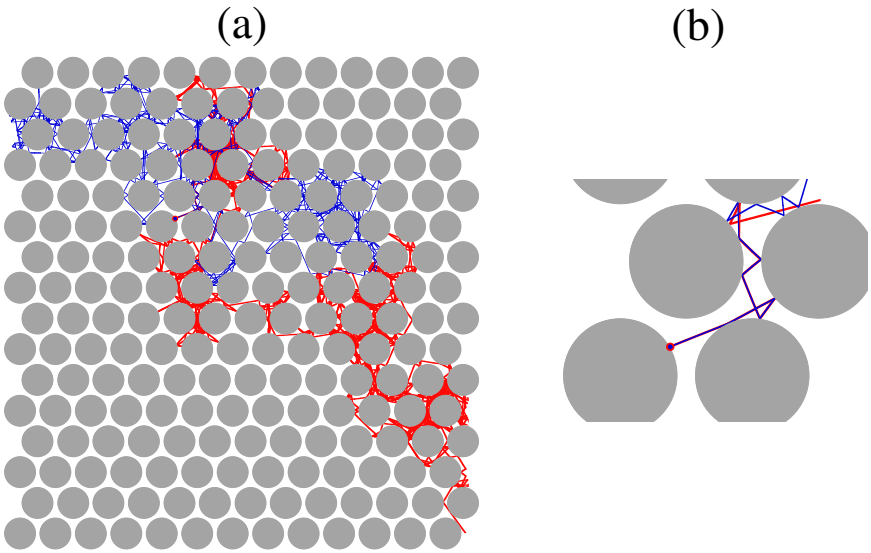

Figure 6. Periodic Lorentz gas in which a point particle undergoes elastic collisions on hard-disk scatterers forming a triangular lattice: (a) Two trajectories of slightly different initial conditions, illustrating the sensitivity to initial conditions and the resulting dynamical randomness. (b) Zoom near the initial positions showing that both trajectories already diverge after eight collisions although the initial conditions only differ by one part in a million.

for hard-disk scatterers of radius a, and

$$V = -\frac{\exp(-\kappa r)}{r} \ , \tag{36}$$

for attractive screened Coulombic scatterers.[69] The chaotic diffusion of both Lorentz gases is illustrated in Figs. 6 and 7. These Hamiltonian flows can be reduced to area-preserving Poincaré mappings by considering the intersections of the trajectory with a surface of section. These Poincaré mappings have been extensively studied.[3,4,15] The multibaker map is a simplification of such Poincaré mappings and, in this regard, it constitutes a model of chaotic diffusion.[3,66]

The periodicity of the potential allows us to introduce a wavenumber $\mathbf{k}$ by the spatial Fourier transform of the density of trajectories. Each Fourier component of the density evolves in time independently of the other components

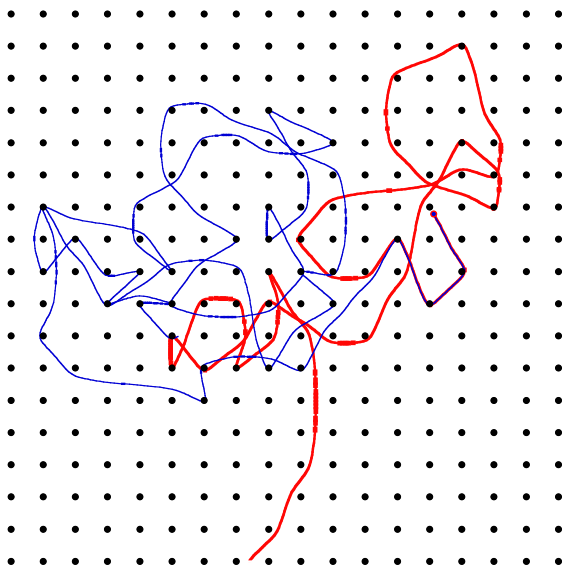

Figure 7. Periodic Lorentz gas in which a charged particle of mass $m = 1$ moves in a square lattice of screened Coulomb potentials with $\kappa = 2$ at energy $E = 3$: Pair of trajectories issued from initial conditions differing by one part in a million, in order to illustrate the chaotic property of this system.

so that, for periodic systems, the Frobenius-Perron operator (17) decomposes into a different operator $\hat{Q}^t_{\mathbf{k}}$ for each value of the wavenumber. Each of these operators may thus have a spectrum of decay rates, i.e., of Pollicott-Ruelle resonances $\{\gamma_{\mathbf{k}}\}$, which depend on the wavenumber $\mathbf{k}$:

$$\hat{Q}^t_{\mathbf{k}} \; \Psi_{\mathbf{k}} = \exp(-\gamma_{\mathbf{k}} t) \; \Psi_{\mathbf{k}} \; . \tag{37}$$

The smallest decay rate controls the long-time hydrodynamic relaxation of the $\mathbf{k}$-component of the density and, accordingly, it gives the dispersion relation of the hydrodynamic modes of diffusion. This dispersion relation is equivalently given in terms of the Van Hove intermediate incoherent scattering function[27,28,70] by

$$\gamma_{\mathbf{k}} = - \lim_{t \to \infty} \frac{1}{t} \ln \langle \exp[i\mathbf{k} \cdot (\mathbf{r}_t - \mathbf{r}_0)] \rangle = \mathcal{D} \; \mathbf{k}^2 + \mathcal{O}(\mathbf{k}^4) \; , \tag{38}$$

where $\mathcal{D}$ is the diffusion coefficient. The eigenstate $\Psi_{\mathbf{k}}$ corresponding to this

smallest decay rate is not a function but a mathematical distribution which has a cumulative function

$$F_{\mathbf{k}}(\theta) = \int_0^\theta d\theta' \; \Psi_{\mathbf{k}}(\mathbf{X}_{\theta'}) \; , \tag{39}$$

where $\mathbf{X}_\theta$ denotes a one-dimensional family of points in phase space. Such cumulative functions have been exactly constructed in the multibaker map, where they are given by de Rham complex functions.[24,63,64,65] The plot of $[\mathrm{Re}\; F_{\mathbf{k}}(\theta), \mathrm{Im}\; F_{\mathbf{k}}(\theta)]$ in the complex plane is a fractal curve having a Hausdorff dimension $0 \leq D_{\mathrm{H}}(\mathbf{k}) \leq 2$ which is determined by the diffusion coefficient $\mathcal{D}$ and by the Lyapunov exponent λ according to

$$\mathcal{D} = \lambda \lim_{\mathbf{k}\to 0} \frac{D_{\mathrm{H}}(\mathbf{k}) - 1}{\mathbf{k}^2} \; , \tag{40}$$

as recently proved for multibaker maps.[30] This formula has a structure very similar to the escape-rate formula (33).

6 Nonequilibrium steady states

Nonequilibrium steady states occur when we consider a fluid of diffusive particles between two reservoirs of particles at different concentrations. This difference of concentration generates a gradient $\mathbf{g} = \nabla \mathbf{c}$. After a relaxation time, a nonequilibrium steady state is established between both reservoirs. For reservoirs separated by a large distance, such steady states can be defined in terms of the long-wavelength hydrodynamic modes according to[25,71]

$$\Psi_{\mathbf{g}}(\mathbf{X}) \;=\; -i \; \mathbf{g} \cdot \frac{\partial \Psi_{\mathbf{k}}(\mathbf{X})}{\partial \mathbf{k}}\Big|_{\mathbf{k}=0} \; . \tag{41}$$

A simple calculation shows that this formula leads to the result[3,44]

$$\Psi_{\mathbf{g}}(\mathbf{X}) \;=\; \mathbf{g} \cdot \left[\mathbf{r}(\mathbf{X}) + \int_0^{-\infty} \mathbf{v}(\mathbf{\Phi}^t \mathbf{X}) \; dt \right] = \Psi_{\mathbf{g}}(\mathbf{\Phi}^t \mathbf{X}) \; , \tag{42}$$

where $(\mathbf{r}, \mathbf{v})$ denote the position and velocity of the particle moving in the lattice. The density (42) is time invariant as expected for a steady state in a system with a constant diffusion coefficient. An average over the distribution of velocities shows that the steady state has a mean linear profile of concentration: $\langle \Psi_{\mathbf{g}} \rangle_{\mathbf{v}} = \mathbf{g} \cdot \mathbf{r}$. However, the fine velocity distribution wildly fluctuates so that the density (42) is not a function but a singular distribution. Its associated cumulative function

$$T_{\mathbf{g}}(\theta) = \int_0^\theta d\theta' \; \Psi_{\mathbf{g}}(\mathbf{X}_{\theta'}) \; , \tag{43}$$

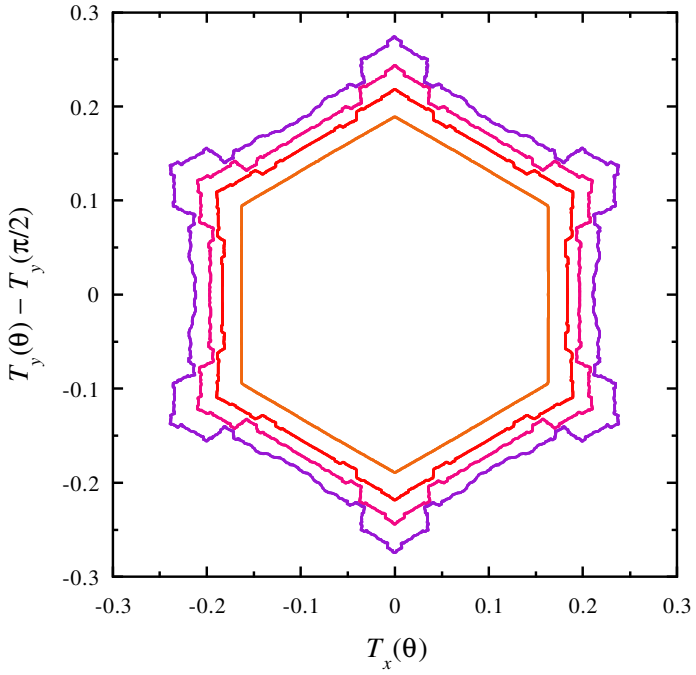

Figure 8. Periodic Lorentz gas in which a point particle undergoes elastic collisions on hard-disk scatterers forming a triangular lattice: The nonequilibrium steady states of the periodic Lorentz gases for distances between the centers of the disks equal to $d = 2.001, 2.1, 2.2, 2.3$ times the disk radius. The plot depicts $T_y(\theta) - T_y(\pi/2)$ versus $T_x(\theta)$, with the integrals Eq. (43) performed over all the initial conditions issued from the border of a disk with a velocity normal to the disk. The initial positions range from a point on the horizontal axis ($\theta = 0$) until a varying point at an angle θ on the border of the disk.

is thus continuous but nondifferentiable.

For the dyadic multibaker map, this cumulative function has been shown to be given by the Takagi function,[71] and this function is indeed known to be continuous but nowhere differentiable. The curve $[\theta, T(\theta)]$ has remarkable self-similar structures with the Hausdorff dimension $D_{\rm H} = 1$.

For the two-dimensional Lorentz gases (34)-(36), the phase-space point $\mathbf{X}_\theta$ in Eq. (43) is taken as a position and a velocity making an angle θ with respect to the x-axis and the gradient of concentration can be considered in

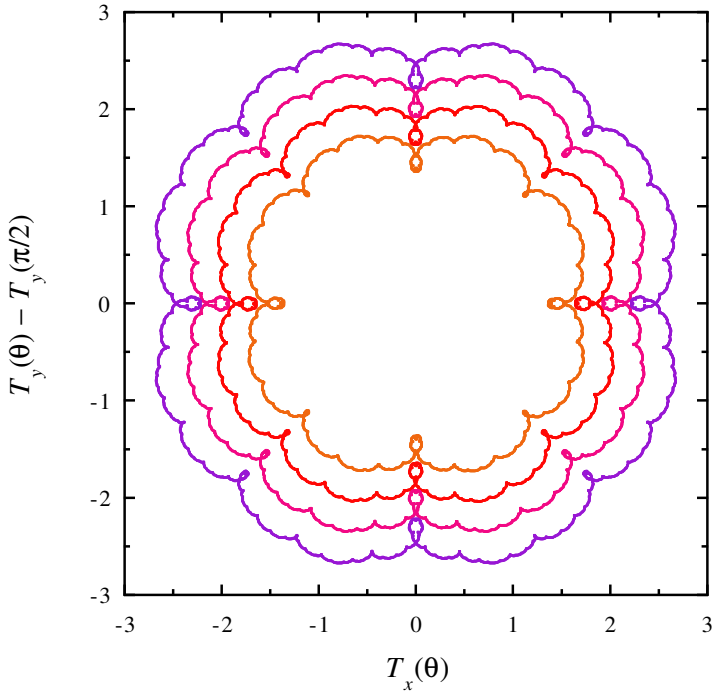

Figure 9. Periodic Lorentz gas in which a charged particle of mass $m = 1$ moves in a square lattice of screened Coulomb potentials (36) with $\kappa = 2$: Cumulative functions of nonequilibrium steady states for a motion at the energies $E = 2, 3, 4, 5$. The plot depicts $T_y(\theta) - T_y(\pi/2)$ versus $T_x(\theta)$, with Eq. (43) integrated over all the initial conditions of a particle starting from the vicinity of a Coulomb center, with a velocity making an angle θ with respect to the x-axis.

the directions x or y. In this way, two generalized Takagi functions $T_x(\theta)$ and $T_y(\theta)$ are defined. The plot of $[T_x(\theta), T_y(\theta) - T_y(\pi/2)]$ is depicted in Figs. 8 and 9 for both Lorentz gases considered. The geometry of these curves is determined by the lattice of the system. For the hard-disk scatterers, the lattice is triangular and the interaction potential is repulsive so that the curve has a hexagonal symmetry and presents protruding self-similar structures. For the screened Coulombic scatterer, the lattice is squared and the potential is attractive so that the curve has a fourfold symmetry and presents intruding structures due to the backscattering of the moving particle upon collision on

each attractive Coulomb center. These fractal curves reveal a very subtle order underlying the chaotic diffusion process over the lattice (compare with Figs. 6 and 7).

The nonequilibrium steady states can also be constructed for the other transport processes.[3,25] A steady state of gradient g associated with the transport property α is given in terms of the corresponding microscopic current $J^{(\alpha)}$ and Helfand moment $G^{(\alpha)}$ by

$$\Psi_g^{(\alpha)}(\mathbf{X}) \;=\; g\;\left[G^{(\alpha)}(\mathbf{X}) + \int_0^{-\infty} J^{(\alpha)}(\mathbf{\Phi}^t\mathbf{X})\;dt\right] = \Psi_g^{(\alpha)}(\mathbf{\Phi}^t\mathbf{X})\;. \qquad (44)$$

Fick's and Fourier's laws are consequences of these steady states because the average microscopic current $J^{(\alpha)}$ is related to the gradient and the transport coefficient by

$$\langle J^{(\alpha)}\rangle_{\rm noneq} \equiv \langle J^{(\alpha)}\Psi_g^{(\alpha)}\rangle_{\rm eq} = -\alpha\;g\;, \qquad (45)$$

which is obtained by Eq. (26) and by noticing that $\langle JG\rangle = \langle (dG/dt)G\rangle = (1/2)(d/dt)\langle G^2\rangle = 0$.

Recently, diffusion-reaction systems have been studied along similar lines and the chemical modes of relaxation have also been constructed.[72,73,74] These chemical modes are also given in terms of singular and fractal distributions without density function.

The singular character of the decay modes which control the hydrodynamics turns out to be a very general property which has nowadays been observed in many different volume-preserving systems. In the next section, we explain why this singular character is so much important for our understanding of the second law of thermodynamics.

7 Fractals and the second law of thermodynamics

According to the second law of thermodynamics, the entropy of a system is either exchanged with the external environment or irreversibly produced inside the system:[75]

$$\frac{dS}{dt} = \frac{d_{\rm e}S}{dt} + \frac{d_{\rm i}S}{dt}\;, \qquad \text{and} \qquad \frac{d_{\rm i}S}{dt} \geq 0\;. \qquad (46)$$

This law is fundamental for hydrodynamics, macroscopic electrodynamics, and chemical or biochemical kinetics. Already, Boltzmann has provided an explanation for this law in terms of the most probable evolution followed by the trajectory of the system between its initial and final conditions. Moreover, Boltzmann's equation is the prototype of a kinetic equation for which a

H-theorem can be proved.[18] However, such kinetic equations have all been obtained by some approximation which introduces a nondeterministic stochastic element which is absent in the original mechanical system even if this latter is chaotic. Accordingly, since Boltzmann's work, a missing link has remained between mechanics and thermodynamics. The discovery of the singular and fractal character of the hydrodynamic modes in volume-preserving chaotic systems fills this gap and provides an explanation for the second law of thermodynamics, which is based on Hamiltonian mechanics and which is thus intrinsic to the dynamics of the system.[29,30]

Indeed, if the long-time relaxation toward the thermodynamic equilibrium state is controlled by a hydrodynamic mode which is a singular distribution and not a smooth distribution, the usual reasoning based on the existence of a density function no longer holds to understand the asymptotic time evolution of the physical observables and, in particular, of the entropy. A step-by-step calculation of the time evolution of the entropy in a multibaker model shows that taking into account the singular character of the hydrodynamic modes makes a fundamental difference: Instead of finding a vanishing entropy production, the obtained value is precisely the one expected from irreversible thermodynamics

$$\frac{d_{\rm i}S}{dt} = \int \mathcal{D}\ \frac{(\nabla c)^2}{c}\ d\mathbf{r}\ , \tag{47}$$

in the limit of a small gradient ∇c of concentration c.[30] The explicit calculation given below shows that the phenomenological value (47) is recovered because the cumulative functions of the hydrodynamic modes and, especially, of the nonequilibrium steady state have some nondifferentiability, i.e., because the distribution is singular.

For the dyadic multibaker map ϕ, the nonequilibrium probability measure evolves in time according to

$$\nu_{t+1}(B) = \nu_t(\phi^{-1}B)\ , \tag{48}$$

where B is a small cell in phase space. The entropy of a phase-space domain A, which is coarse-grained into cells $\{B\}$, is defined by

$$S_t(A:\{B\}) = \sum_{B\subset A} \nu_t(B)\ \ln\frac{\mu(B)}{\nu_t(B)}\ , \tag{49}$$

where μ is the invariant equilibrium measure. Under the discrete-time evolution of the map, the entropy changes in time because of two contributions:

$$\Delta S_t \equiv S_{t+1} - S_t = \Delta_{\rm e}S_t + \Delta_{\rm i}S_t\ . \tag{50}$$

These contributions are the entropy flux

$$\Delta_{\rm e} S_t \equiv S_t(\phi^{-1}A : \{B\}) - S_t(A : \{B\}) \ , \tag{51}$$

and the entropy production

$$\Delta_{\rm i} S_t = S_{t+1}(A : \{B\}) - S_{t+1}(A : \{\phi B\}) \ , \tag{52}$$

resulting from Eqs. (50)-(51) and the identity $S_t(\phi^{-1}A : \{B\}) = S_{t+1}(A : \{\phi B\})$.

Let us suppose that the cells B are of size Δy where y is the phase-space coordinate in the direction of the stable manifolds where the fractal structure of the hydrodynamic modes develops. It has been shown that the nonequilibrium measure of the cell B can be expanded in powers of the mean gradient of concentration $g_t = \nabla c_t$ according to[29,30,71]

$$\nu_t(B) = c_t + g_t \left[T(y + \Delta y) - T(y) \right] + \mathcal{O}(g_t^2) \ , \tag{53}$$

where $T(y)$ is the continuous and nondifferentiable Takagi function which is solution of the following recursive equation[71]

$$T(y) = \begin{cases} \frac{1}{2} T(2y) + y \ , & 0 < y < \frac{1}{2} \ , \\ \frac{1}{2} T(2y-1) + 1 - y \ , & \frac{1}{2} < y < 1 \ . \end{cases} \tag{54}$$

The nondifferentiability of the Takagi function implies that its second difference vanishes linearly as $\Delta y \to 0$:[29]

$$2\, T\left(y + \frac{\Delta y}{2} \right) - T(y + \Delta y) - T(y) = \Delta y \ , \tag{55}$$

instead of quadratically which is the crucial step to obtain a positive entropy production. Indeed, the gradient expansion of the theoretical entropy production (52) shows that

$$\Delta_{\rm i} S_t = \sum_{\rm cells} \frac{g_t^2}{2 c_t \Delta y} \left[2\, T\left(y + \frac{\Delta y}{2} \right) - T(y + \Delta y) - T(y) \right]^2 + \cdots \ , \tag{56}$$

in a unit square A of the multibaker. Thanks to the property (55) and the fact that the number of cells in the sum is equal to $(1/\Delta y)$, we find that the theoretical entropy production coincides with the phenomenological entropy production

$$\Delta_{\rm i} S_t = \frac{1}{\Delta y} \, \frac{g_t^2}{2 c_t \Delta y} \, \Delta y^2 + \cdots = \mathcal{D} \, \frac{(\nabla c_t)^2}{c_t} + \cdots \ , \tag{57}$$

(up to higher-order terms in the gradient) because the diffusion coefficient of the dyadic multibaker map is $\mathcal{D} = 1/2$.

If the hydrodynamic mode was given by a regular distribution, the Takagi function (which is a cumulative function) would be differentiable and its second difference (55) would vanish as Δy^2. Hence the theoretical entropy production (57) would also vanish as Δy^2 in the limit $\Delta y \to 0$ of arbitrarily fine coarse graining, which would be a contradiction with respect to the phenomenological entropy production (47). In the simple example of the multibaker map, the second law is therefore a direct consequence of the singular and fractal character of the hydrodynamic modes which control the asymptotic relaxation toward the equilibrium state. We notice that the result holds for arbitrarily fine coarse-graining. Accordingly, the result is essentially independent of the coarse-graining and is robust in this regard. The result extends to other chaotic systems as well.

8 Conclusions and perspectives

Recent progress in nonequilibrium physics has shown that exponential relaxation toward the thermodynamic equilibrium proceeds via hydrodynamic modes which are singular and fractal. The singular property is a consequence of the dynamical instability in the microscopic dynamics (see Subsec. 3.4) while the fractal property is a consequence of the dynamical randomness, i.e., of the microscopic chaos in the dynamics of particles. On this basis, it has been possible to derive the second law of thermodynamics. In this regard, it turns out that the second law of thermodynamics has a fractal origin.

In the derivation carried out in Sec. 7, the second law is a consequence of the spectral decomposition (20) of the Frobenius-Perron operator and of the fact that its eigenstates are singular distributions without density function. For dynamically unstable systems such as the chaotic systems, the time evolution splits into a forward semigroup valid for $0 < t < +\infty$ and a backward semigroup for $-\infty < t < 0$. The eigenstates of the forward semigroup are singular in the stable phase-space directions and regular in the unstable directions and *vice versa* in the case of the backward semigroup. The splitting of the time evolution into two semigroups is a spontaneous breaking of the time-reversal symmetry due to the dynamical instability. This symmetry breaking occurs at the statistical level of description. The positive entropy production (57) holds for the forward semigroup and is thus a result of the spontaneous symmetry breaking. For the backward semigroup the entropy production would be negative but the present theory shows that such anti-thermodynamic behaviour will never occur during the lapse of time $0 < t < +\infty$. Indeed, the backward semigroup is not valid for $0 < t < +\infty$ because its spectral decomposition does not converge for the positive times.[3] Therefore, the use of the

backward semigroup is restricted by a fundamental horizon at the origin of time $t = 0$ when the initial density is given. This fundamental horizon is a consequence of the spontaneous breaking of the time-reversal symmetry and it limits the range of applicability of thermodynamics to evolutions from the present toward the future. In chaotic systems, the time-reversal symmetry turns out to be spontaneously broken at the statistical level of description, which can explain how the irreversible behaviour of thermodynamics emerges out of a microscopically reversible dynamics of particles.

Since the key of the previous reasoning is the analytic continuation of the Liouvillian resolvent toward complex frequencies where the Pollicott-Ruelle resonances lie, the previous explanation is very similar to Gamow's explanation of exponentially decaying quantum states.[2] An important difference with respect to quantum systems is that, in classical mechanics, such exponentially decaying states can only be defined in terms of singular distributions. Fig. 10 depicts three famous examples of probability distributions. The first one is the familar Gaussian distribution which is regular since its density is the well-known bell-shaped function. The next example is the Cantor singular distribution without density function. Its cumulative function is known as the devil staircase which has a zero derivative almost everywhere but is nevertheless increasing because its derivative is infinite on Cantor's set. Therefore, the singularities of the density are concentrated on a fractal set of zero probability on the unit interval. Such distributions appear in the escape-rate formalism in which the invariant set is a fractal repeller. The third example is the Lebesgue singular distribution without density function but only a cumulative function.[76] In this last example, the singularities of the density are dense in the unit interval as it is the case for the hydrodynamic modes and the nonequilibrium steady states of infinite systems without escape. For long time, the relevance of such singular distributions to nonequilibrium physics has remained uncertain but recent work has shown that they play a fundamental role to explain the most subtle aspects of statistical mechanics.

One of the major preoccupations of nonequilibrium physics is to understand the time-dependent phenomena and explain the various observed time-dependence such as dynamical chaos, exponential decay, power-law decay, finite-time collapse or blow-up, etc... Work in this field is revealing the growing importance of transient and unstable processes, which we referred to as ephemeral phenomena in the Introduction. We notice that the stable structures which are observed in Nature are the result of dynamical evolutions in which the ephemeral phenomena have manifested themselves. Dynamical perturbations of the stable structures reactivate these unstable and transient processes, which points out that the stable structures emerge out of a vast

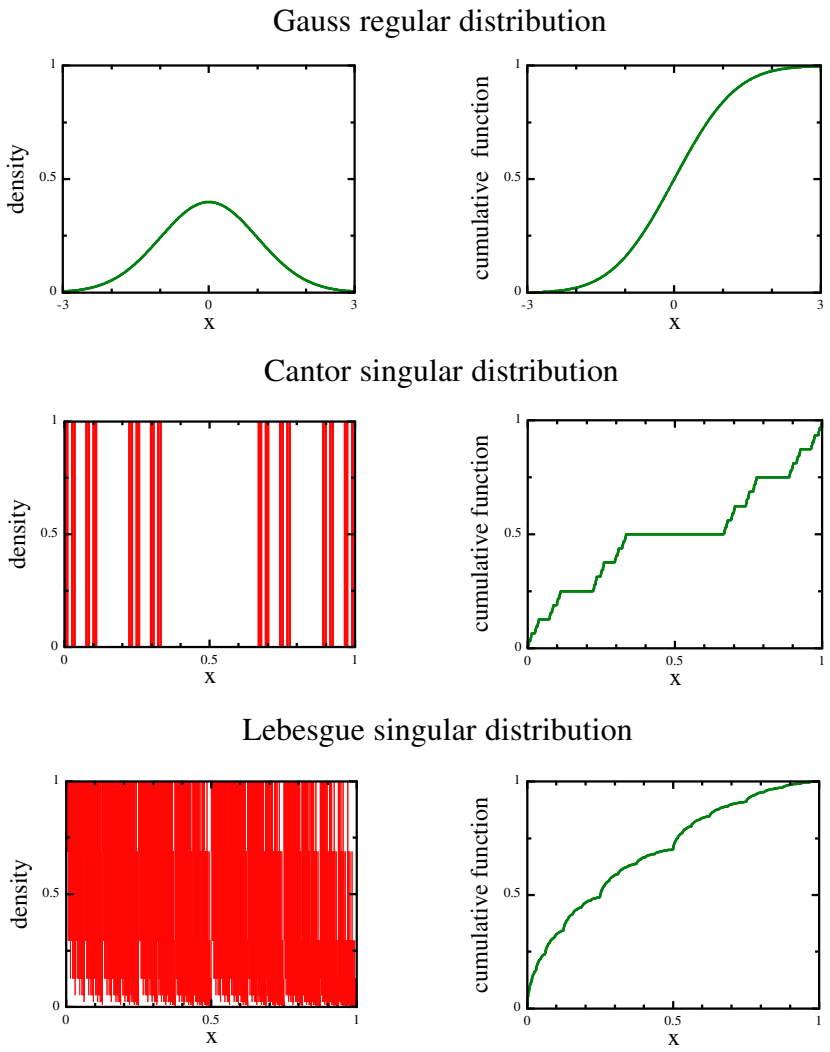

Figure 10. Three important examples of probability distributions.

majority of ephemeral phenomena. Progress in our understanding of the stable structures thus requires the study of ephemeral phenomena on shorter

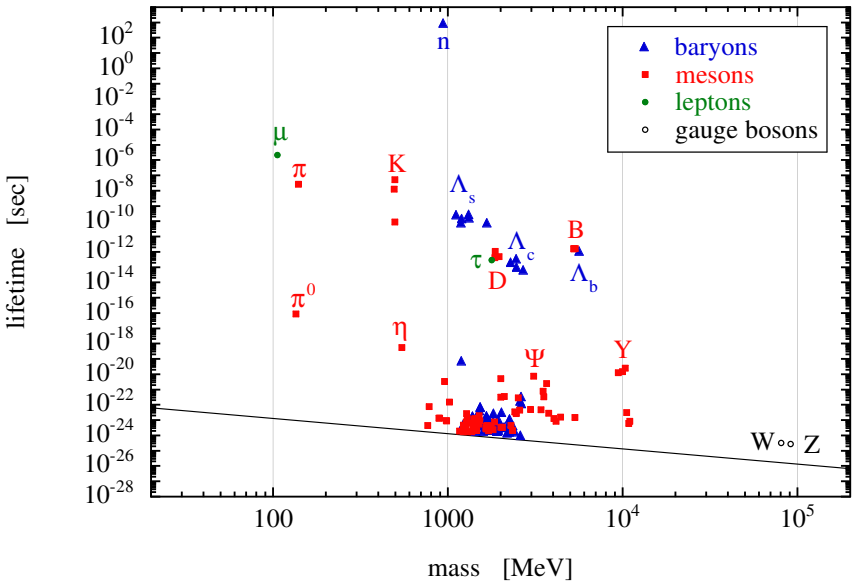

Figure 11. Lifetime $\tau = \hbar/\Gamma$ versus mass m for the known fundamental particles. The oblique line represents the observational limit of resonances of widths $\Gamma = m/2$ which are so wide that they disappear into the continuous background. The electron and the proton do not appear because they are stable.

and shorter time scales. This is the case in the study of thermodynamics and transport processes, as summarized in this paper. The concept of dynamical instability is also at the basis of the theory of far-from-equilibrium patterns such as Turing patterns.[15,77,78,79] The interest for ephemeral phenomena is also the trend in chemical kinetics with the advent of femtochemistry allowing to study and control chemical reactions on the time scale of the internal motion of molecules.[80,81,82] In order to illustrate how general this trend can be, we have plotted in Fig. 11 the lifetime of high-energy particles versus their mass.[83] As their mass increases, their lifetime tends to decrease. Yet, the particles of the highest masses are fundamental to explain the long-lived particles at lower masses. Similarly, the understanding of atomic nuclei has required the study of unstable and short-lived nuclei, which are the parents of the stable nuclei. In this perspective, the stable structures of matter are the result of unstable and transient processes, which appears as a physical

principle of evolution. The dynamical instability performs a kind of selection of the stablest among all the possible particles and structures of matter.

It is striking how general such a principle of evolution can be since it extends apparently from fundamental physics to the other natural sciences such as chemistry, geology, and biology. In this discussion, we think that it is worthwhile to emphasize the similarities which could exist with the principle of biological evolution where the concepts of transient phenomena and of selection also play essential roles. Far from being independent disciplines, all the natural sciences acquire a unity in the perspective given by the recent advances in nonequilibrium and nonlinear science.

Acknowledgments

The author thanks Professor G. Nicolis for support and encouragement in this research. The "Fonds National de la Recherche Scientifique" (FNRS Belgium) is gratefully acknowledged for financial support. This work has also been financially supported by the Université Libre de Bruxelles and the InterUniversity Attraction Pole Program of the Belgian Federal Office of Scientific, Technical and Cultural Affairs.

References

1. C. J. Joachain, *Quantum Collision Theory* (North-Holland, Amsterdam, 1975).
2. A. Bohm, *Quantum Mechanics* (Springer, New York, 1979).
3. P. Gaspard, *Chaos, Scattering and Statistical Mechanics* (Cambridge University Press, Cambridge UK, 1998).
4. J.-P. Eckmann and D. Ruelle, *Rev. Mod. Phys.* **57**, 617 (1985).
5. N. N. Krylov, *Nature* **153**, 709 (1944); N. N. Krylov, *Works on the Foundations of Statistical Mechanics* (Princeton University Press, 1979); Ya. G. Sinai, *ibid.* p. 239.
6. Ya. G. Sinai, *Russian Math. Surveys* **25**, 137 (1970).
7. P. Gaspard and G. Nicolis, *Physicalia Magazine (J. Belg. Phys. Soc.)* **7**, 151 (1985).
8. R. Livi, A. Politi, and S. Ruffo, *J. Phys. A: Math. Gen.* **19**, 2033 (1986).
9. H. A. Posch and W. G. Hoover, *Phys. Rev. A* **38**, 473 (1988).
10. Ch. Dellago, H. A. Posch, and W. G. Hoover, *Phys. Rev. E* **53**, 1485 (1996).
11. H. van Beijeren and J. R. Dorfman, *Phys. Rev. Lett.* **74**, 4412 (1995); **76**, 3238 (1996).

12. H. van Beijeren, J. R. Dorfman, H. A. Posch, and Ch. Dellago, *Phys. Rev. E* **56**, 5272 (1997).
13. N. I. Chernov, *J. Stat. Phys.* **88**, 1 (1997).
14. R. van Zon, H. van Beijeren, and Ch. Dellago, *Phys. Rev. Lett.* **80**, 2035 (1998).
15. G. Nicolis, *Introduction to Nonlinear Science* (Cambridge University Press, Cambridge UK, 1995).
16. D. J. Evans, E. G. D. Cohen, and G. Morriss, *Phys. Rev. A* **42**, 5990 (1990).
17. P. Gaspard and G. Nicolis, *Phys. Rev. Lett.* **65**, 1693 (1990).
18. J. R. Dorfman, *An Introduction to Chaos in Nonequilibrium Statistical Mechanics* (Cambridge University Press, Cambridge UK, 1999).
19. C. P. Dettmann, *The Lorentz gas as a paradigm for nonequilibrium stationary states*, in: D. Szasz, Editor, *Hard Ball Systems and Lorentz Gas*, Encycl. Math. Sci. (Springer, Berlin, 2000).
20. T. Gilbert, J. R. Dorfman, and P. Gaspard, *Fractal dimensions of the hydrodynamic modes of diffusion*, (preprint `nlin.CD/0007008`, server `xxx.lanl.gov`).
21. P. Gaspard and F. Baras, *Phys. Rev. E* **51**, 5332 (1995).
22. J. R. Dorfman and P. Gaspard, *Phys. Rev. E* **51**, 28 (1995).
23. P. Gaspard and J. R. Dorfman, *Phys. Rev. E* **52**, 3525 (1995).
24. P. Gaspard, *Chaos* **3**, 427 (1993).
25. P. Gaspard, *Phys. Rev. E* **53**, 4379 (1996).
26. R. Balescu, *Equilibrium and Nonequilibrium Statistical Mechanics* (Wiley, New York, 1975).
27. P. Résibois and M. De Leener, *Classical Kinetic Theory of Fluids* (Wiley, New York, 1977).
28. J.-P. Boon and S. Yip, *Molecular Hydrodynamics* (Dover, New York, 1980).
29. P. Gaspard, *J. Stat. Phys.* **88**, 1215 (1997).
30. T. Gilbert, J. R. Dorfman, and P. Gaspard, *Phys. Rev. Lett.* **85**, 1606 (2000).
31. Matthieu Louis, *Chaos Microscopique dans un Modèle de Mouvement Brownien* (Mémoire de licence en sciences physiques, Université Libre de Bruxelles, 1999).
32. A. N. Kolmogorov, *Dokl. Acad. Sci. USSR* **119**(5), 861 (1958); **124**(4), 754 (1959); Ya. G. Sinai, *Dokl. Acad. Sci. USSR* **124**(4), 768 (1959).
33. V. I. Arnold and A. Avez, *Ergodic Problems of Classical Mechanics* (W. A. Benjamin, New York, 1968).
34. C. E. Shannon and W. Weaver, *Mathematical Theory of Communication*

(The University of Illinois Press, Urbana, 1949).
35. H. Kantz and P. Grassberger, *Physica D* **17**, 75 (1985).
36. N. I. Chernov and R. Markarian, *Boletim da Sociedade Brasileira de Matemática* **28**, 271, 342 (1997).
37. Ya. B. Pesin, *Math. USSR Izv.* **10**(6), 1261 (1976); *Russian Math. Surveys* **32**(4), 55 (1977).
38. P. Gaspard and X.-J. Wang, *Phys. Rep.* **235**, 291 (1993).
39. P. Gaspard, M. E. Briggs, M. K. Francis, J. V. Sengers, R. W. Gammon, J. R. Dorfman, and R. V. Calabrese, *Nature* **394**, 865 (1998).
40. A. Connes, H. Narnhofer, and W. Thirring, *Commun. Math. Phys.* **112**, 691 (1987).
41. R. Alicki and M. Fannes, *Lett. Math. Phys.* **32**, 75 (1994).
42. P. Gaspard, *Prog. Theor. Phys. Suppl.* **116**, 369 (1994); P. Gaspard, in: J. Karkheck, Editor, *Dynamics: Models and Kinetic Methods for Non-Equilibrium Many Body Systems*, NATO ASI Series (Kluwer, Dordrecht, 2000) pp. 425-456.
43. I. Prigogine, *Nonequilibrium Statistical Mechanics* (Wiley, New York, 1962).
44. P. Gaspard, *Physica A* **240**, 54 (1997).
45. M. Pollicott, *Invent. Math.* **81**, 413 (1985).
46. M. Pollicott, *Invent. Math.* **85**, 147 (1986).
47. D. Ruelle, *Phys. Rev. Lett.* **56**, 405 (1986).
48. D. Ruelle, *J. Stat. Phys.* **44**, 281 (1986).
49. D. Ruelle, *J. Diff. Geom.* **25**, 99, 117 (1987).
50. D. Ruelle, *Commun. Math. Phys.* **125**, 239 (1989).
51. P. Cvitanović and B. Eckhardt, *J. Phys. A: Math. Gen.* **24**, L237 (1991).
52. R. Artuso, E. Aurell, and P. Cvitanović, *Nonlinearity* **3**, 325, 361 (1990).
53. P. Cvitanović, R. Artuso, F. Christiansen, P. Dahlqvist, R. Mainieri, H. H. Rugh, G. Tanner, G. Vattay, N. Whelan, and A. Wirzba, *Classical and Quantum Chaos* (`http://www.nbi.dk/ChaosBook/`).
54. P. Gaspard and D. Alonso Ramirez, *Phys. Rev. A* **45**, 8383 (1992).
55. W. Lu, L. Viola, K. Pance, M. Rose, and S. Sridhar, *Phys. Rev. E* **61**, 3652 (2000); K. Pance, W. Lu, and S. Sridhar, *Phys. Rev. Lett.* **85** (2000).
56. I. Gel'fand and G. Shilov, *Generalized Functions*, Vol. 2 (Academic Press, New York, 1968).
57. N. Dunford and J. T. Schwartz, *Linear operators*, Vols. I-III (Interscience-Wiley, New York, 1958, 1963, 1971).
58. P. D. Lax and R. S. Phillips, *Scattering Theory* (Academic Press, New York, 1967).

59. E. Helfand, *Phys. Rev.* **119**, 1 (1960).
60. M. S. Green, *J. Chem. Phys.* **20**, 1281 (1952); **22**, 398 (1954).
61. R. Kubo, *J. Phys. Soc. Jpn.* **12**, 570 (1957).
62. I. Claus and P. Gaspard, *Fractals and dynamical chaos in a 2D reactive Lorentz gas with sinks* (preprint, Université Libre de Bruxelles, 2000).
63. S. Tasaki, I. Antoniou, and Z. Suchanecki, *Phys. Lett. A* **179**, 97 (1993).
64. H. H. Hasegawa and D. J. Driebe, *Phys. Rev. E* **50**, 1781 (1994).
65. D. J. Driebe, *Fully Chaotic Maps and Broken Time Symmetry* (Kluwer, Dordrecht, 1999).
66. P. Gaspard, *J. Stat. Phys.* **68**, 673 (1992).
67. L. A. Bunimovich and Ya. G. Sinai, *Commun. Math. Phys.* **78**, 247, 479 (1980).
68. N. I. Chernov, *J. Stat. Phys.* **74**, 11 (1994).
69. A. Knauf, *Commun. Math. Phys.* **110**, 89 (1987); A. Knauf, *Ann. Phys. (N. Y.)* **191**, 205 (1989).
70. L. Van Hove, *Phys. Rev.* **95**, 249 (1954).
71. S. Tasaki and P. Gaspard, *J. Stat. Phys.* **81**, 935 (1995).
72. P. Gaspard and R. Klages, *Chaos* **8**, 409 (1998).
73. P. Gaspard, *Physica A* **263**, 315 (1999).
74. I. Claus and P. Gaspard, *Microscopic chaos and reaction-diffusion processes in the periodic Lorentz gas*, *J. Stat. Phys.* **101** (2000).
75. I. Prigogine, *Introduction to the Thermodynamics of Irreversible Processes* (Wiley, New York, 1961).
76. S. Tasaki, T. Gilbert, and J. R. Dorfman, *Chaos* **8**, 424 (1998).
77. M. C. Cross and P. C. Hohenberg, *Rev. Mod. Phys.* **65**, 851 (1993).
78. F. Baras and M. Malek Mansour, *Adv. Chem. Phys.* **100**, 393 (1997).
79. A. De Wit, *Adv. Chem. Phys.* **109**, 435 (1999).
80. A. H. Zewail, *Femtochemistry*, Vols. I-II (World Scientific, Singapore, 1994).
81. P. Gaspard and I. Burghardt, Editors, *Chemical Reactions and their Control on the Femtosecond Time Scale*, Proceedings of the XXth Solvay Conference on Chemistry, *Adv. Chem. Phys.* **101** (1997).
82. S. A. Rice and M. Zhao, *Optical Control of Molecular Dynamics* (Wiley, New York, 2000).
83. R. M. Barnett *et al.* (Particle Data Group), *Rev. Mod. Phys.* **68**, 611 (1996).

International Journal of Modern Physics B **15** (2001) 209-235;
also in:
Louis H. Y. Chen, J. Packer Jesudason, C. H. Lai, C. H. Oh, K. K. Phua & Eng-Chye Tan, Eds., *Challenges for the 21st Century, Proceedings of the International Conference on Fundamental Sciences: Mathematics and Theoretical Physics, Singapore, 13-17 March 2000* (World Scientific, Singapore, 2001) pp. 398-429.